Report of the Mount Haleakala Observatory

AN ATMOSPHERIC LIDAR DATA-ACQUISITION SYSTEM USING AN ON-LINE DIGITAL COMPUTER

PAUL D. McCORMICK

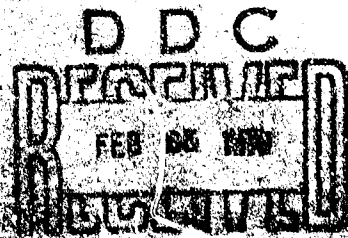H. DAVID HULTQUIST

February 1970

DDC

FEB

NOTICES

Sponsorship. The work reported herein is a part of the research under Project AMOS conducted at the Willow Run Laboratories of the Institute of Science and Technology for the Advanced Research Projects Agency, Department of Defense, under Contract DAHC-15-68-C-0144. Contracts and grants to The University of Michigan for the support of sponsored research are administered through the Office of the Vice-President for Research.

Project Description. A primary objective of Project AMOS is the determination of the usefulness of ground-based optics for tracking and measuring the physical parameters of space objects. Other objectives include measuring geophysical parameters and conducting observation programs at the Mount Haleakala Observatory in selected areas of infrared astronomy. The Mount Haleakala Observatory is located on Kole Kole Peak, Mount Haleakala, on the island of Maui, Hawaii. The facility is operated by a staff of engineers, astrophysicists, and technicians, who maintain the station and conduct all long-term observations and experiments.

Project AMOS utilizes the capabilities of the Computation Department and of the Radar and Optics Laboratory of Willow Run Laboratories, as well as those of the Department of Electrical Engineering in the College of Engineering and the Department of Astronomy in the College of Literature, Science, and the Arts of The University of Michigan.

Distribution. Initial distribution is indicated at the end of this document.

Final Disposition. After this document has served its purpose, it may be destroyed. Please do not return it to the Willow Run Laboratories.

1386-29-T

Report of the Mount Haleakala Observatory

AN ATMOSPHERIC LIDAR DATA-ACQUISITION SYSTEM USING AN ON-LINE DIGITAL COMPUTER

PAUL D. McCORMICK

H. DAVID HULTQUIST

February 1970

Willow Run Laboratories
THE INSTITUTE OF SCIENCE AND TECHNOLOGY
THE UNIVERSITY OF MICHIGAN
Ann Arbor, Michigan

ACKNOWLEDGMENTS

ABSTRACT

This report describes the design and operation of a data-acquisition system which uses digital circuits and an on-line PDP-8/I computer for real-time data processing to make upper atmospheric LIDAR measurements. The system is presently being used with the high-power pulsed ruby laser which has recently been installed at the Mount Haleakala Observatory, Maui, Hawaii.

The report discusses the basic concepts involved in obtaining LIDAR measurements of atmospheric backscattering. Expected signal returns for both the "current" (lower atmosphere) and pulse-counting (upper atmosphere) cases are calculated. Noise and background sources are considered in detail, and the statistical nature of the upper atmospheric experiments is emphasized. Detailed circuit diagrams for the data-acquisition system and a LIDAR data-acquisition program for the PDP-8/I computer are also included.

Preliminary data obtained with the LIDAR system is presented and compared with prediction. It is concluded that the Mount Haleakala LIDAR system will be capable of producing high-precision atmospheric backscattering profiles to altitudes of the order of 100 km.

———————— WILLOW RUN LABORATORIES ————————

CONTENTS

FIGURES

TABLES

AN ATMOSPHERIC LIDAR DATA-ACQUISITION
SYSTEM USING AN ON-LINE DIGITAL COMPUTER

INTRODUCTION

Several of the inherent properties of pulsed ruby lasers serve to make them an almost ideal
source of radiation for atmospheric scattering measurements. Large energy outputs produce
detectable returns from the upper atmosphere. Short pulse lengths allow altitude resolution to
be determined by the detection system or the detection statistics rather than by the laser. The
fact that the radiation is almost spatially coherent permits the use of relatively small diameter
collimating optics to achieve transmitted beam divergences of the order of tenths of milliradians.
Since the radiation is also almost temporally coherent, narrowband interference filters may be
inserted in front of the detector to reduce the effect of sky background. It is, therefore, not sur-
prising that several experimental groups have been actively engaged in atmospheric studies with
pulsed ruby lasers for the past several years [1-6].

This relatively new technique for atmospheric studies (given the name LIDAR for Light
Detection and Ranging) measures directly an atmospheric parameter, called the differential scat-
tering function, which involves products of particle concentrations and scattering cross sections.
In the case of scattering by particulate matter, integrals over particle size distributions are in-
cluded. Most of the LIDAR systems presently in operation utilize a boresighted transmitter and
(separate) receiver. The University of Maryland uses a single optical path for transmitting and
receiving [5]. All of these systems are, therefore, restricted to a measurement of the differen-
tial backscattering function.

One or two groups have constructed LIDAR systems in which the transmitter and receiver
are separated by tens of kilometers in order to measure the scattering function at angles other
than 180°.

The exponential dependence of atmospheric density upon altitude causes the atmosphere to
separate into two regions from the standpoint of signal level. Below a certain altitude, the re-
turn consists of a photoelectron current and may be displayed on an oscilloscope. Above this
altitude, the return is so weak that single photoelectron counting is required. Assuming a typical
laser system and reasonable values for other parameters, the transition altitude is somewhere
near 40 km.

Early LIDAR systems used oscilloscope photography for data display, and Northend et al.
[7] have described such a system in detail. Although single photoelectron counting is possible

with oscilloscope photography, this technique is tedious and time consuming. An obvious solution to the problem is the use of digital pulse-counting techniques.

This report describes the design, calibration and performance of a data-acquisition system which uses digital circuits and an on-line PDP-8/I computer for real-time data processing to make upper atmosphere LIDAR measurements. The system is presently in use with the high-power pulsed ruby laser which has recently been installed at the Mount Haleakala Observatory, Maui, Hawaii. The data-acquisition system is similar to one that was used by one of the authors with The University of Maryland's optical radar [5].

2
A LIDAR SYSTEM FOR BOTH LOWER AND UPPER ATMOSPHERIC STUDIES

Figure 1 illustrates the basic components of the Mount Haleakala LIDAR system, which can be used for both lower (below 30 km) and upper atmospheric measurements. The ruby laser is operated in the Q-switched mode (pulse lengths of the order of 50 nsec) and fired through a collimating telescope. The output may be several joules per pulse into a beam angle of the order of tenths of milliradians.

Backscattered radiation is collected by the receiver, brought to a focus (where apertures defining the field of view may be inserted), recollimated, and passed through a narrowband interference filter to the cathode of a photomultiplier (e.g., EMI 9558A).

Two rotating shutters are installed, one in front of the laser output ruby to prevent fluorescence from escaping into the atmosphere, and one in front of the photomultiplier to prevent overloading due to the high returns produced by backscattering in the lower atmosphere. (The shutters are particularly necessary when probing the upper atmosphere with the pulse-counting system.) The use of these shutters is discussed in more detail in a later section. Since the laser pulse must be fired through the rotating fluorescence shutter, synchronization signals and electronic delays are provided as shown in the figure.

"Current" signals (from the lower atmosphere) are displayed on an oscilloscope and photographed. A logarithmic amplifier is normally used because of the large dynamic range of the signal.

Single photoelectron counting (due to backscattering from the upper atmosphere) is accomplished by the remaining components of the system and it is these components—i.e., photomultiplier (PMT), pulse amplifiers, pulse height discriminator, control logic, interface, computer—that are of primary interest in this report.

It should be emphasized that the two types of measurements are incompatible and cannot be done simultaneously. As has been mentioned, a shutter is required in front of the PMT for the
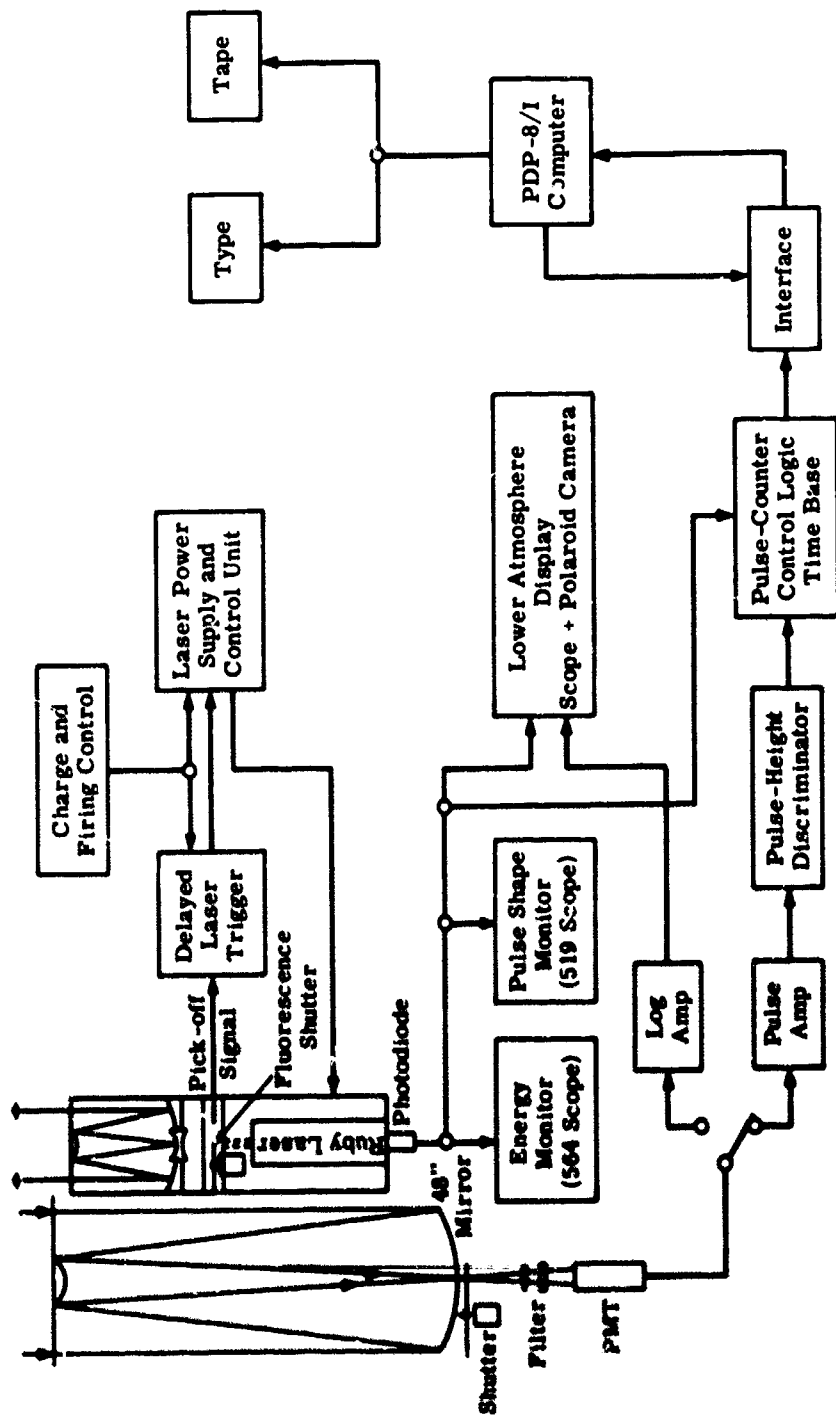
FIGURE 1. THE MOUNT HALEAKALA LIDAR SYSTEM

3

pulse-counting case (this is discussed in detail in sec. 4.3). Mechanical considerations preclude measurements below approximately 20-30 km. For measurements below these altitudes, the shutter is left "open" and oscilloscope photography is utilized. Depending on the system parameters, neutral-density filters may or may not be required.

3
EXPECTED SIGNAL DUE TO MOLECULAR BACKSCATTERING

3.1. LOWER ATMOSPHERE

When the lower atmosphere is probed, the return consists of a photoelectron current, as stated previously. The magnitude of this current at the anode of the photomultiplier as a function of altitude (or time) will be:

$$i_a(z) = \frac{\kappa \alpha_r \tau_\lambda^2(\theta) A_r S_\lambda G(V) E_o c}{2} \cdot \frac{1}{z^2} \cdot \sum_i n_i(z) \sigma_{\omega i}(\pi) \text{ amp} \tag{1}$$

In this expression:

κ = a cuton factor to account for the fact that the boresighted transmitter and receiver are not colinear ($0 \leqq \kappa < 1$)

α_r = optical efficiency of the receiver

$\tau_\lambda(\theta)$ = one-way transmission of the atmosphere for a zenith angle θ and for wavelength λ (6943 Å for ruby at "room" temperature)

A_r = effective collecting area of the receiver

S_λ = cathode radiant sensitivity (amp/W)

$G(V)$ = gain of the photomultiplier at a bias voltage V

E_o = output energy of the laser

c = velocity of light

z = altitude

$n_i(z)$ = concentration of scattering centers (m^{-3}) of type i at altitude z

$\sigma_{\omega i}(\pi)$ = differential backscattering cross section (m^2-sr^{-1}) of a particle of type i

In order to estimate the magnitude of the signal we assume that α_r = 0.3, $\tau \cong 1$, A_r = 1 m^2, S_λ = 1.5 × 10^{-2} amp/W, $G \cong 10^6$, and E_o = 10 J. For a pure molecular atmosphere [$\sigma_\omega(\pi)$ = 2 × 10^{-32} m^2-sr^{-1}] we have:

$$i_a(z) \cong 1.4 \times 10^{-19} \cdot \frac{\kappa(z)n(z)}{z^2} \text{ amp} \tag{2}$$

4

κ is a function of the transmitter and receiver beam angles, the separation between the transmitter and receiver mirrors, and the diameter of the transmitter. The expression is complicated and will not be given here. Values of $\kappa(z)$ for the special case where the transmitter beam angle is 0.1 mrad, the receiver field of view is 0.2 mrad, the transmitter diameter is 0.75 m and the transmitter-receiver mirror separation is 0.35 m are given in table I. Also shown in table I are values of $n(z)$ taken from the U. S. Standard Atmosphere: 1962 [8] and $i_a(z)$ calculated from (2). It is assumed that the LIDAR system is located at sea level.

TABLE I. EXPECTED ANODE CURRENT DUE TO MOLECULAR BACKSCATTERING

z (km)	n(z) (m^{-3})	$\kappa(z)$	$i_a(z)$ (mamp)
1	2.31×10^{25}	0.00	0.000
2	2.09×10^{25}	0.00	0.000
2.3	2.03×10^{25}	0.00	0.000
3	1.89×10^{25}	0.06	17.700
5	1.53×10^{25}	0.24	20.500
7	1.23×10^{25}	0.44	15.500
12	6.49×10^{24}	0.75	4.740
17	2.96×10^{24}	0.95	1.360
21.6	1.43×10^{24}	1.00	0.430
25	8.33×10^{23}	1.00	0.190
30	3.83×10^{23}	1.00	0.060
35	1.76×10^{23}	1.00	0.020
4C	8.31×10^{22}	1.00	0.007
45	4.09×10^{22}	1.00	0.003

Note: a 10-J/pulse laser output is assumed.

Figure 2 is a plot of the values given in table I. It is quite obvious that a large dynamic range in signal is involved (hence the advantage of a logarithmic amplifier). Of course, if the receiver field of view were made larger, then the beams would overlap at lower altitudes, producing very large peak signals and necessitating the use of neutral-density filters to protect the photomultiplier. In figure 2, this effect is illustrated. Also shown is the "envelope" of the various signal curves (i.e., assuming that complete beam overlap is at z = 0).

It is also seen that the return is down to 3×10^{-6} amp at 45 km. This is equivalent to a photomultiplier counting rate of 20 MHz and, therefore, is close to the transition between the "current" and the "pulse-counting" modes.

(1) $\theta_T = 0.1$ mrad
     $\theta_R = 0.2$ mrad

(2) $\theta_T = 0.1$ mrad
     $\theta_R = 0.6$ mrad

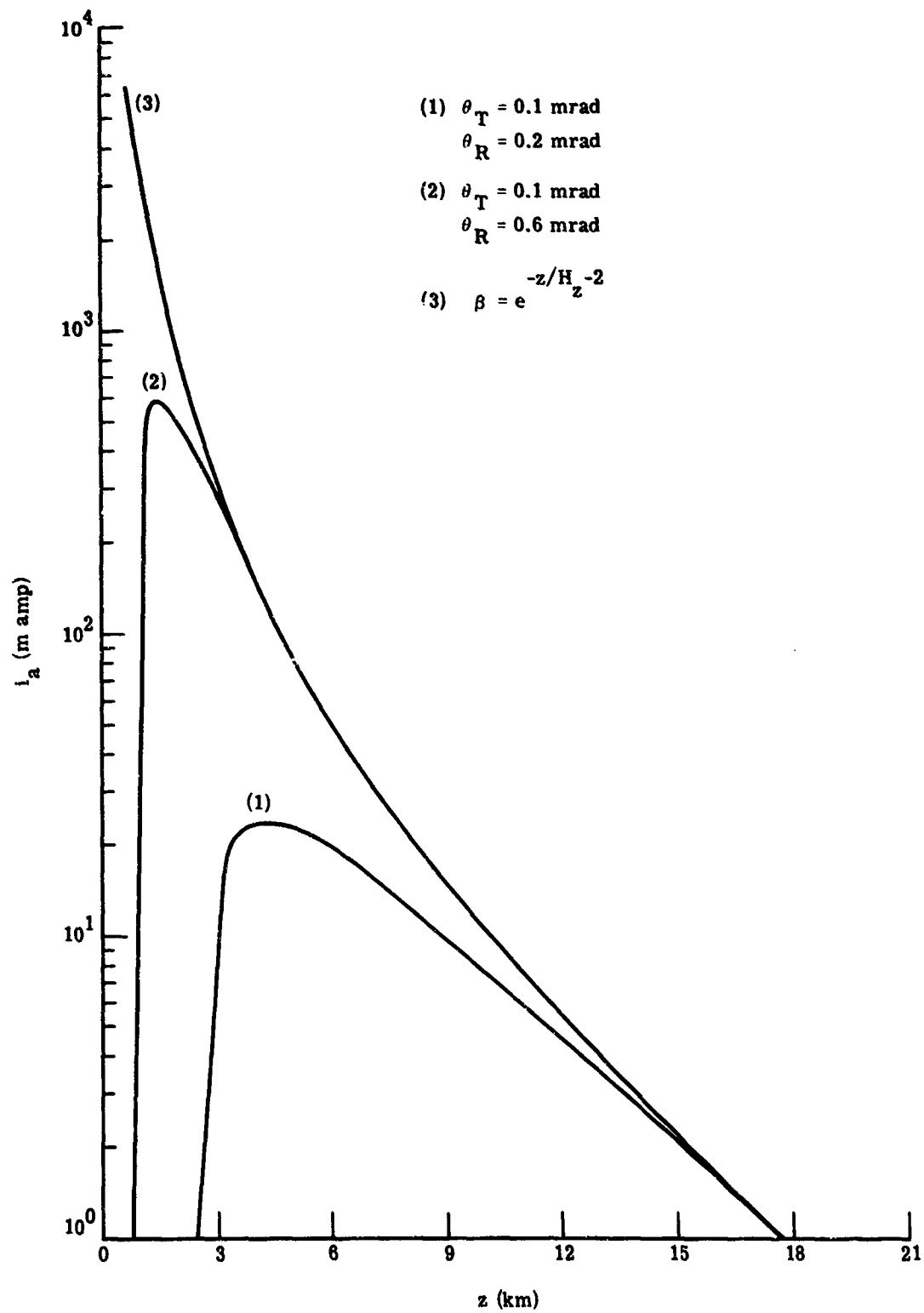(3) $\beta = e^{-z/H_z - 2}$

FIGURE 2. EXPECTED ATMOSPHERIC RETURN

6

3.2. UPPER ATMOSPHERE (PULSE COUNTING)

For the pulse-counting case, equation 1 is better expressed in the following form [5] (we assume that the beams are completely overlapped at these altitudes):

$$N_T(z) = \frac{T\alpha_r Q \tau_\lambda^2(\theta) A_r \lambda E_o}{2h} \cdot \frac{1}{z^2} \cdot \sum_i n_i(z)\sigma_{\omega i}(\pi) \text{ counts in T sec} \tag{3}$$

In this case:

$N_T(z)$ = the number of photoelectron pulses, counted in an interval of T sec, corresponding to backscattered photons originating in a layer $ct/2$ meters thick at an altitude of z meters

Q = the quantum efficiency of the photomultiplier at wavelength λ

h = Planck's constant (6.6×10^{-34} J-sec)

The other quantities in (3) have been previously defined. Assuming that $Q = 0.03$ for $\lambda =$ 6943 Å (consistent with $S_\lambda = 1.5 \times 10^{-2}$ amp/W) and using the same values for the other parameters as was done for the lower atmosphere case, we formulate (4):

$$N_T(z) = 9.4 \times 10^{-7} \cdot \frac{n(z)T}{z^2} \text{ counts in T sec} \tag{4}$$

This expression has been used to calculate the values given in table II. The last column in table II is for $T = 1.6 \times 10^{-5}$ sec since the digital interface discussed in section 5.4 uses this value for the sample time.

An inspection of table II again serves to emphasize the dynamic range involved. At $z \cong 45$ km, we begin to approach the pulse-counting case (i.e., the PMT output becomes resolvable into single photoelectron pulses). One laser firing would produce about 300 counts in a 16-μsec interval centered on a time corresponding to returns from this altitude (45 km). It is assumed, of course, that the width of the PMT pulses is sufficiently narrow for this counting requirement. At $z \cong 80$ km, we expect about one count per laser firing in a 16-μsec interval. About 2×10^3 laser pulses are required before a single count would be expected from 120 km in a 16-μsec interval. It is clear that noise, background, and statistics will play an important part in any upper atmospheric LIDAR experiment.

4
NOISE, BACKGROUND, AND STATISTICS

Several sources of noise and background must be considered when making LIDAR measurements of upper atmospheric backscattering. These are: photomultiplier dark current, enhanced photomultiplier noise produced by the high light levels backscattered from the lower atmosphere,

TABLE II. EXPECTED PULSE COUNT DUE TO MOLECULAR BACKSCATTERING

z (km)	$n(z)$ m^{-3}	$N_T(z)/T$ (counts/sec)	$N_T(z)$ (counts in 16 μsec)
30	3.83×10^{23}	4.0×10^8	6.4×10^3
35	1.76×10^{23}	1.4×10^8	2.2×10^3
40	8.31×10^{22}	4.9×10^7	7.8×10^2
45	4.09×10^{22}	1.9×10^7	3.0×10^2
50	2.14×10^{22}	8.1×10^6	1.3×10^2
55	1.17×10^{22}	3.6×10^6	5.8×10^1
60	6.36×10^{21}	1.7×10^6	2.7×10^1
65	3.46×10^{21}	7.7×10^5	1.2×10^1
70	1.82×10^{21}	3.5×10^5	5.6×10^0
75	9.01×10^{20}	1.5×10^5	2.4×10^0
80	4.16×10^{20}	6.1×10^4	9.8×10^{-1}
85	1.65×10^{20}	2.2×10^4	3.5×10^{-1}
90	6.59×10^{19}	7.6×10^3	1.2×10^{-1}
95	2.52×10^{19}	2.6×10^3	4.2×10^{-2}
100	1.04×10^{19}	9.8×10^2	1.6×10^{-2}
105	4.43×10^{18}	3.8×10^2	6.1×10^{-3}
110	2.07×10^{18}	1.6×10^2	2.6×10^{-3}
115	9.83×10^{17}	7.1×10^1	1.1×10^{-3}
120	5.23×10^{17}	3.4×10^1	5.4×10^{-4}

Note: A 10-J/pulse laser output is assumed.

sky background radiation, electronic noise, direct backscattering of ruby fluorescence and multiple scattering effects.

4.1. PHOTOMULTIPLIER DARK CURRENT

For the EMI 9558A PMT assumed for this experiment (2-in.-diameter S-20 cathode), the dark current should be less than about 20 counts/sec when the tube is cooled to about dry ice temperatures. From table II, we see that this count rate will not be significant until altitudes above about 120 km are reached.

4.2. SKY BACKGROUND

For the sky background spectral radiance near $\lambda = 6943$ Å, we take [9]:

$$R_N = 10^{-9} \text{ W-m}^{-2}\text{-sr}^{-1}\text{-Å}^{-1} \text{ (dark night sky)}$$

$$R_D = 10^{-3} \text{ W-m}^{2}\text{-sr}^{-1}\text{-Å}^{-1} \text{ (day sky—not "near" sun)}$$

Using these values, and the system parameters assumed previously, we may construct table III.

TABLE III. SKY BACKGROUND VS. RECEIVER FOV AND FILTER BANDWIDTH

Receiver FOV (mrad)	Filter Bandpass Å	Counts per Second (Night Sky)	Counts per Second (Day Sky)
0.2	1	1×10^0	1×10^6
	10	1×10^1	1×10^7
	50	5×10^1	5×10^7
0.4	1	4×10^0	4×10^6
	10	4×10^1	4×10^7
	50	2×10^2	2×10^8
0.6	1	9×10^0	9×10^6
	10	9×10^1	9×10^7
	50	5×10^2	5×10^8

Comparing the values given in table III with the predicted return for a 10-J pulse (table II) we note the following:

(a) Atmospheric probing to about 100 km is possible, during dark night sky conditions, even with a 50-Å filter and a 0.6-mrad receiver field of view.

(b) Atmospheric probing to about 60 km is possible during day sky conditions only if very narrowband filters (e.g., 1 Å) and narrow receiver fields of view (e.g., 0.2 mrad) are used.

We will consider these points further in section 4.6. It should be pointed out here, however, that the "minimum detectable signal" (or the "maximum attainable altitude") will, of course, be a function of the number of laser firings used to build up an atmospheric profile.

4.3. ENHANCED PHOTOMULTIPLIER NOISE

When a photomultiplier is exposed to a very intense light source, the dark-current emission may be enhanced for a considerable time afterwards. The actual reason for this behavior is not completely understood.

Not only will an increased dark-current count rate reduce the "maximum attainable altitude," but any large (sporadic) fluctuations might be erroneously interpreted as returns from, perhaps, "dust layers" in the atmosphere. As was shown in section 3.1, very high light levels will be produced by backscattering from the lower atmosphere. It is for this reason that the rotating shutter mentioned previously must be used. The shutter should completely block the photomultiplier during, and for up to about 100 μsec after, the laser firing. This technique allows the LIDAR system to be operated at maximum sensitivity for probing the upper atmosphere. The shutter, ideally, should be completely open by a time corresponding to returns from about 40 km so that the problem of determining a "shutter cuton curve" can be omitted.

4.4. RUBY FLUORESCENCE

A recent paper by one of the authors [10] discusses this subject in detail. It is found that ruby fluorescence will be the most troublesome and significant source of noise for a LIDAR system operated during night sky conditions.

The expression for the expected count rate n as a function of z, due to fluorescence F escaping into the atmosphere after the Q-switched laser pulse, is [10].

$$n_F(z) = \frac{cK}{2H} \int_{z_0/H}^{z/H} \frac{e^{-x}}{x^2} dx \text{ counts/sec} \qquad (5)$$

where H = atmospheric density scale height

z_0 = altitude where the transmitter and receiver beams overlap (a step function overlap is assumed for simplicity)

x = z/H

and

$$K = \tau_a^2 \alpha_r Q V A_r n_0 \sigma(\pi) n_i \theta_r^2 d_T^2 \Big/ 6ctd_L^2 \beta$$

in which V = volume of ruby

n_i = number of chromium ions per unit volume

n_0 = sea-level molecular concentration

d_T = diameter of the transmitting telescope

d_L = diameter of the output ruby

10

t = fluorescence lifetime of ruby

β = a parameter describing the "collimation" of the fluorescence from the output ruby
   $(0 < \beta \leqq 1)$

θ_r = receiver field of view

The other parameters have been previously defined. For altitudes above about 40 km, it turns out that n_F is essentially independent of z [10]. Table IV gives values of n_F as a function of θ_r and β. Also included are values of z_o for the system parameters listed under the table. It is assumed that the overlap is zero below z_o and complete above z_o. This means that the values for n_F given in table IV are upper limits from the standpoint of the parameter z_o alone.

A comparison of the values for n_F (table IV) to those for N_T/T (table II) clearly demonstrates the potential contamination of atmospheric returns by ruby fluorescence. It is also obvious that the altitude level at which the noise due to fluorescence is equal to the signal expected due to atmospheric backscattering is strongly dependent upon the LIDAR system parameters and on

TABLE IV. EXPECTED COUNT RATE DUE TO RUBY FLUORESCENCE (z > 40 km)

β	θ_r (mrad)	z_o (km)	n_F (counts/sec)
1.0	0.2	2.0	2.5×10^5
	0.4	1.5	1.8×10^6
	0.6	1.0	4.3×10^6
0.5	0.2	2.0	5.0×10^5
	0.4	1.5	3.6×10^6
	0.6	1.0	8.6×10^6
0.1	0.2	2.0	2.5×10^6
	0.4	1.5	1.8×10^7
	0.6	1.0	4.3×10^7

$\theta_T = 0.1$ mrad $\qquad n_1 = 1.6 \times 10^{25}$ m^{-3}

$\tau_a = 1$ $\qquad d_T = 0.74$ m

$\alpha_r = 0.3$ $\qquad \tau = 3 \times 10^{-3}$ sec

$Q = 0.03$ $\qquad d_L = 0.02$ m

$V = 10^{-4}$ m^3 $\qquad H = 8 \times 10^3$ m

$A_r = 1$ m^2 $\qquad \sigma(\pi) = 2 \times 10^{-32}$ m^{-2}-sr^{-1}

$n_o = 2.5 \times 10^{25}$ m^{-3}

$d = 0.34$ m = separation between transmitter and receiver mirrors

the collimation of the fluorescence leaving the output ruby. For z_o = 2.0 km and β = 1 (fluorescence emitted into 2π sr) the "crossover altitude" is somewhere near 70 km, while for z_o = 1.0 km and β = 0.1 it is about 40 km.

Although several approximations were used in the derivation of (5) (see ref. 10), it is clear that ruby fluorescence must be prevented from entering the atmosphere after the Q-switched pulse, if backscattering measurements are to be made from very high altitudes. The usual method of doing this is to install a rotating shutter in front of the output ruby. (Reference 10 also discusses the requirements on shutter cutoff times in order to prevent spurious "layers" from being generated.)

4.5. MULTIPLE SCATTERING

Bettinger [11] has analyzed the possible effects of multiple scattering in detail. His results indicate that, except for very unusual physical situations, multiple scattering would not be a significant source of noise below altitudes of about 150 km for a LIDAR system such as the one described in this report.

4.6. STATISTICAL CONSIDERATIONS

Table II shows that the expected return from the upper atmosphere is very low if only molecular scattering is present. This requires that noise and background contributions be minimized and suggests that statistical analysis (of an elementary sort) will play a rather large part in data reduction. In this section, the ability of a LIDAR system to detect molecular and/or aerosol scattering in the upper atmosphere is calculated.

Consider a particular layer at altitude z, where each layer represents T sec of integration time, and sum the result of K laser firings. The total number of observed counts can be written as $KTn_o(z)$, where $n_o(z)$ is the effective count rate (in photoelectrons per second) and is assumed to be constant over T sec (i.e., a "stratified" atmosphere is assumed). $n_o(z)$ is also averaged over the K laser firings because, in order to study possible time variations in the backscattering, K should be as small as possible, consistent with other criteria to be mentioned below.

If $n_s(z)$ is the unknown signal (molecular and/or aerosol scattering) count rate for this layer and n_n is the noise count rate, then:

$$KTn_o(z) = KT[n_s(z) + n_n]$$

It is assumed that n_n includes all sources of noise and background (PMT dark current, night sky, etc.), is constant in time, and is determined by an independent measurement. The assumption of constancy in time for n_n implies that no laser-related noise (e.g., fluorescence) is present. The independent measurement of n_n consists of a continuous monitor between laser firings and the inspection of the computer printout for very high altitudes (e.g., greater than 150

12

km). The noise measurements are made over a time $t_n \gg KT$ so that the uncertainty in the mean value of n_n can be made very small. To be specific, suppose that the noise has been measured for a time t_n and, therefore, $n_n t_n$ counts have been observed. The noise count rate is:

$$n_n \pm \left(\frac{n_n}{t_n}\right)^{1/2} \text{ counts/sec}$$

The uncertainty in the measurement of $KTn_c(z)$ will be:

$$\{KT[n_s(z) + n_n]\}^{1/2}$$

The derived value of signal count rate is, then:

$$n_s(z) = n_0(z) - n_n \pm \left[\frac{n_s(z) + n_n}{KT} + \frac{n_n}{t_n}\right]^{1/2}$$

In order to give a more precise meaning to the word "uncertainty," it should be mentioned that the sampling process is assumed to be described by Poisson statistics.

If $t_n \gg KT$ then the n_n/t_n term can be neglected. Therefore:

$$n_s(z) = n_0(z) - n_n \pm \left[\frac{n_s + n_n}{KT}\right]^{1/2}$$

It is useful to express the above result in terms of counts per interval (T sec).

Let: $N_s(z) = Tn_s(z) = $ signal counts/interval

$N_0(z) = Tn_0(z) = $ observed counts/interval

$N_n = Tn_n = $ noise counts/interval

The result is:

$$N_s(z) = N_0(z) - N_n \pm \left[\frac{N_s(z) + N_n}{K}\right]^{1/2} = N_0(z) - N_n \pm \left[\frac{N_0(z)}{K}\right]^{1/2} \tag{6}$$

$N_s(z)$ is identical to $N_T(z)$ (eq. 3) and represents the number of signal counts per interval per shot when an atmospheric profile has been determined from an average of K laser firings. $N_s(z)$ is obtained from the computer printout using equation 6, and then $n(z)\sigma_\omega(\pi)$ is calculated using equation 3. The fractional error in $n(z)\sigma_\omega(\pi)$ will be equal to the fractional error in $N_s(z)$.

Consider the following cases:

(1) Suppose that it is desired to detect molecular scattering with a confidence of about 95%. This requires that $N_s(z)$ be approximately 2 noise standard deviations above the mean noise level.

$$N_s(z) = 2(N_n/K)^{1/2}$$

From the results given in previous sections, a typical value for N_n might be about 60 counts/sec (PMT dark current plus night sky) for $\theta_r = 0.4$ mrad and $\Delta\lambda = 10$ Å. This results in $N_n \cong 10^{-3}$ counts/interval. Suppose we want to sum the result of 100 shots. Then:

$$N_s(z) = 6.3 \times 10^{-3} \text{ counts/interval}$$

From table II, this value of $N_s(z)$ would correspond to an altitude of $z \cong 105$ km for an energy output of 10 J/pulse. In other words, if 100 shots (at 10 J/shot) are fired and the only source of backscattering is due to the molecular concentration predicted by the 1962 U. S. Standard Atmosphere, then the signal in the 100-km bin will exceed the expected noise level by 2 noise standard deviations. (This "signal" would be 1 count on every other 100 shot "trial.")

(2) In Case 1, a measurement of the molecular scattering with some specified degree of precision is necessary. Consider the requirement that the ratio of the uncertainty in a measurement of $N_s(z)$ to the measured mean value of $N_s(z)$ be some fraction f. Statistically this means that molecular scattering is measured to (100f)% with a 70% level of confidence, since 1 standard deviation is used as the uncertainty. An alternative interpretation would be that molecular scattering is measured to $(100 \times 2f)$% with a 95% level of confidence. (These statements are true for samples drawn from a normally distributed population.)

$$\left[\frac{N_s(z) + N_n}{K}\right]^{1/2} = f \cdot N_s(z)$$

Solving for K:

$$K = \frac{1}{f^2} \frac{N_s(z) + N_n}{N_s^2(z)} \tag{7}$$

If, for example, $f = 0.1$ (molecular scattering is to be measured to $\pm 10\%$), $N_n = 10^{-3}$ counts/interval and the value of $N_s(z)$ for a 10-J pulse and an altitude of 50 km (table II) is used, the

14

result is K ≅ 1 shot. The system, therefore, can measure molecular scattering from 50 km to better than ±10% with each shot, assuming that the other parameters in equation 3 are known with this precision. It should be pointed out that, if the atmospheric profile can be fitted to the predicted molecular curve in a particular altitude region, then ±1% measurements or better are possible on a short-time (hourly) basis. It has been found, for example, that the returns from near 50 km follow the predicted exponential curve very closely [5]. If the observations are scaled to fit in this region, high-precision measurements can be justified. The only parameter in equation 3 that is likely to fluctuate on a short-term basis (aside from n_σ at a particular altitude) is the atmospheric transmission.

Consider, for example, the 100-km level. It would require about 10^3 shots (about 0.6 hr of observation time at 1 pulse per 2 sec) to measure molecular scattering to ±25%. No other LIDAR group has published data that approaches this capability. (The parameters assumed in this report, although not representing actual capabilities or specifications, are reasonable to assume for the Mount Haleakala LIDAR system.) It should also be pointed out that the system parameters used in the calculations are not necessarily upper limits, and an increase in energy output, repetition rate, and efficiency (for example, by the multiple-pass quantum enhancement technique) could easily increase the sensitivity per hour by an order of magnitude.

Figure 3 is a plot of equation 7 for several values of f. This figure shows how many shots are required to measure molecular scattering to a given precision, as a function of altitude, for a 10-J laser pulse. The background is assumed to be 10^{-2} counts per 16-μsec interval. As is shown in the figure, the PMT quantum efficiency is assumed to be 0.03 (at 6943 Å) for the first three curves. This value is representative of "off-the-shelf" S-20 PMT's. Recently, tubes have become available with quantum efficiencies as high as 0.08 at 6943 Å. If a tube with optical quantum enhancement is employed, resultant quantum efficiencies of about 0.15 may be expected. Such a system was assumed in the final curve.

Of particular interest is the possible accumulation of aerosols at the mesopause. McCormick et al. [4] reported the observation of a differential backscattering function about 20 times the expected molecular value from about 80 km. They required approximately 300 laser pulses at 2 J/pulse (2.5 hr at 2 pulses/min) to measure this enhancement to ±50%. The Mount Haleakala LIDAR system (including the expected molecular scattering as noise) can measure this aerosol concentration (±50%) with about 4 shots. This is a very important capability since there are indications that, with a time scale of the order of 1 hr, variations in the aerosol concentration are present.
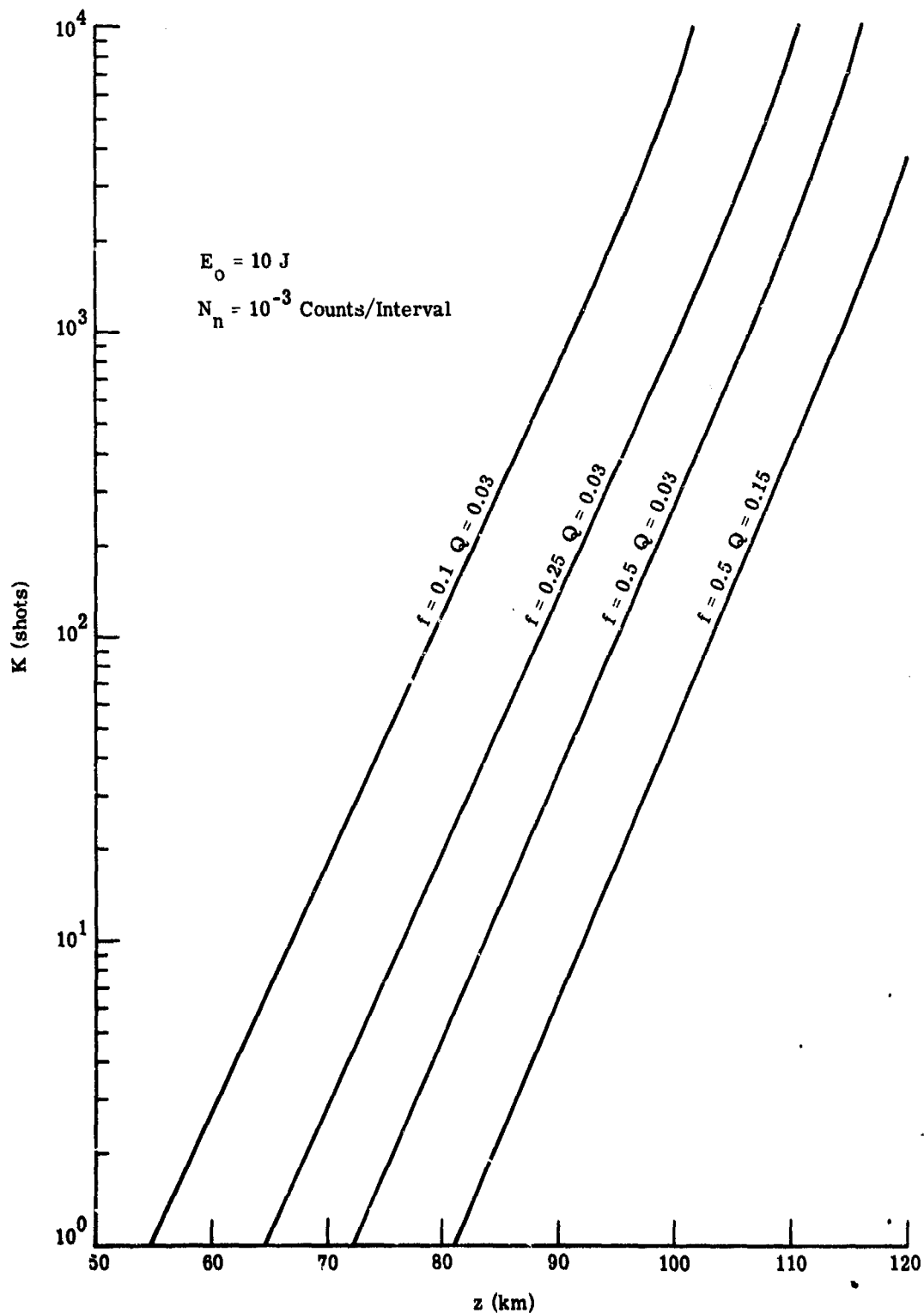
FIGURE 3. NUMBER OF SHOTS NEEDED TO MEASURE MOLECULAR SCATTERING

16

5
DESCRIPTION OF THE DATA-ACQUISITION SYSTEM

Previous sections of this report have been fairly general and would apply to essentially any LIDAR system. This section describes, in detail, the particular data-acquisition system that is presently in use at the Mount Haleakala Observatory. The basic components are shown in figure 4.
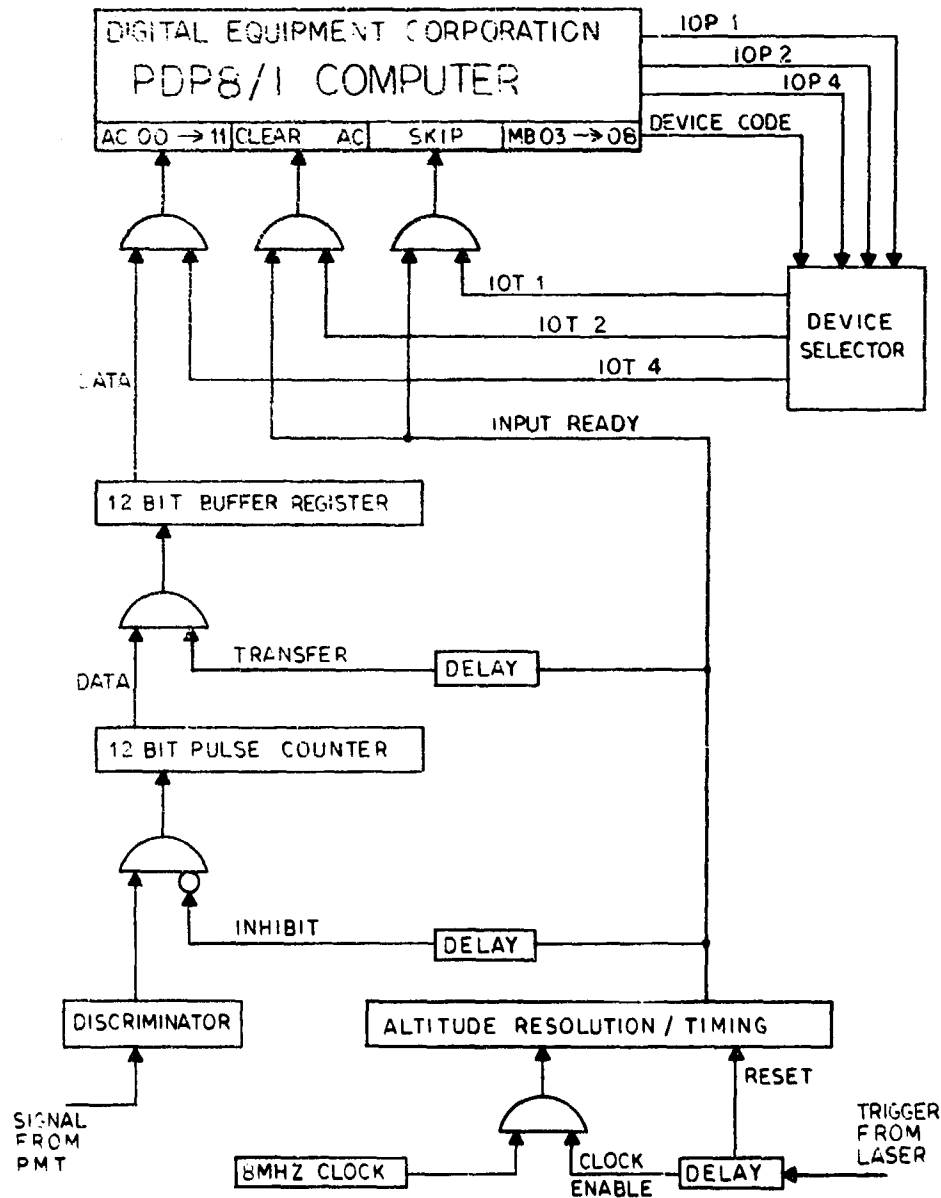
FIGURE 4. LIDAR INTERFACE BLOCK DIAGRAM

5.1. DETECTOR

The detector is an EMI 9558A photomultiplier tube. The gain of this tube is the order of 10^6 to 10^7 under typical operating conditions. The spectral response is S-20 and the quantum efficiency is about 0.05 at 6943 A.

5.2. PULSE AMPLIFIERS

Photoelectron pulses from the photomultiplier are amplified by two or three stages of EG&G type AN 101 pulse amplifiers (each amplifier has a gain of 4). The rise time of these amplifiers is about 2.2 nsec, the recovery time is about 2.5 nsec, and the (linear) input ampli-tude range is from +10 to -100 mV.

5.3. PULSE-HEIGHT DISCRIMINATION

Since the pulse-height distribution of photoelectrons is different from that of the dark cur-rent, pulse-height discrimination is possible. The output of the pulse amplifiers is sent to an EG&G TR 104S/N pulse-height discriminator (-100 to -600 mV in 100-mV steps). The standard output pulse of the discriminator is then sent to the digital interface described below.

Reference 5 discusses techniques for determining the correct settings of PMT bias voltage, external amplification, and discriminator level to insure that essentially all (e.g., 95%) of the photoelectron pulses are counted, while the majority of the dark-current pulses are rejected.

5.4. DIGITAL INTERFACE

Pulses from the discriminator are sent to the digital interface shown in figure 4. The purpose of the interface is to process the incoming photoelectron pulses into a form suitable for direct input to an on-line PDP-8/I computer. The basic operation of the interface is de-scribed below. Details are included in the appendix. All components of the interface are Dig-ital Equipment Corp. Flip Chip Modules.

The photoelectron pulses first enter a 12-bit pulse counter. The first two stages of the pulse counter are 10-MHz flip-flops while the rest can operate at up to 2 MHz. PMT pulses are counted continuously except when an inhibit pulse (to be discussed later) is applied to the gate shown in the figure.

When the laser is fired, a trigger pulse is applied to the CLOCK ENABLE one-shot multi-vibrator as shown. The output of this one-shot gates pulses from an 8.0-MHz crystal oscillator into a 7-bit counter (labeled ALTITUDE RESOLUTION/TIMING), which uses 10-MHz flip-flops for the first three stages and 2-MHz flip-flops for the remaining four stages. The width of the output pulse from the one-shot sets the total altitude range over which atmospheric returns will be accepted (e.g., 1 msec for 150 km).

18

The last stage of the 7-bit counter makes a 0 to 1 (or a 1 to 0) transition every 16 μsec (with the first transition occurring 8 μsec after the laser fires). This is the time that determines the altitude resolution of the LIDAR system (2.4 km for 16 μsec). (See figure 5 for a detailed timing diagram.) The 1 to 0 transition performs two functions: it inhibits discriminator pulses from being counted for approximately 0.5 μsec (by using the one-shot shown in the figure), and alerts the transfer gates (for about 0.1 μsec) so that the "instantaneous" pulse count may be jam transferred into the 12-bit buffer register. The inhibit pulse is necessary to insure that a pulse-counter flip-flop is not changing its state when a buffer transfer is taking place. It is seen, therefore, that the contents of the pulse counter are transferred to the buffers every 16 μsec as long as clock pulses are being gated into the 7-bit counter.

The "1" level which is designated INPUT READY and exists, of course, for 8 μsec before a 1 to 0 transition, alerts one side of the SKIP and CLEAR gates. During the 8-μsec interval that these gates are alerted, data may be transferred to the accumulator of the PDP-8/I under program control.

5.5. PDP-8/I COMPUTER

A Digital Equipment Corporation (DEC) PDP-8/I computer is used, on-line with the Mount Haleakala LIDAR system. In order to understand the following paragraphs it is necessary to be familiar with DEC's Small Computer Handbook [12] and Logic Handbook [13].

When the PDP-8/I comes to an IOT (Input-Output-Transfer) instruction, the computer goes into an expanded 4.25-μsec cycle. During this period three negative-going pulses may be produced by the computer and are available at three output pins. These pulses are designated IOP 1, IOP 2 and IOP 4, and are produced according to the value of the least significant bit of the basic machine language octal IOT instruction. The basic octal instruction has the form 6YYX, where the "6" initiates the expanded computer cycle, the "YY" will be the device code (some octal number), and the "X" specifies the number of IOP pulses produced. If X = 7 all three IOP pulses are available. These pulses are each -3 V in amplitude and 400 nsec wide. IOP 1 comes approximately 1.25 μsec after the expanded cycle is entered, and IOP 2 and IOP 4 follow IOP 1 by 1.0 μsec and 2.0 μsec respectively. The IOP pulses are used to effect data transfers to and from external equipment. If the PDP-8/I receives a SKIP pulse (at the appropriate pin) during the IOT period, it will skip the next instruction. (The contents of the PDP-8/I program counter will be incremented by 1.) Therefore, a simple way to effect a data input is to have an IOT instruction followed by a Jump-1 instruction. The computer will remain in a "skip-loop" until the SKIP pin is activated—at which time it will skip the Jump-1 instruction and enter, e.g., the data storage routine.
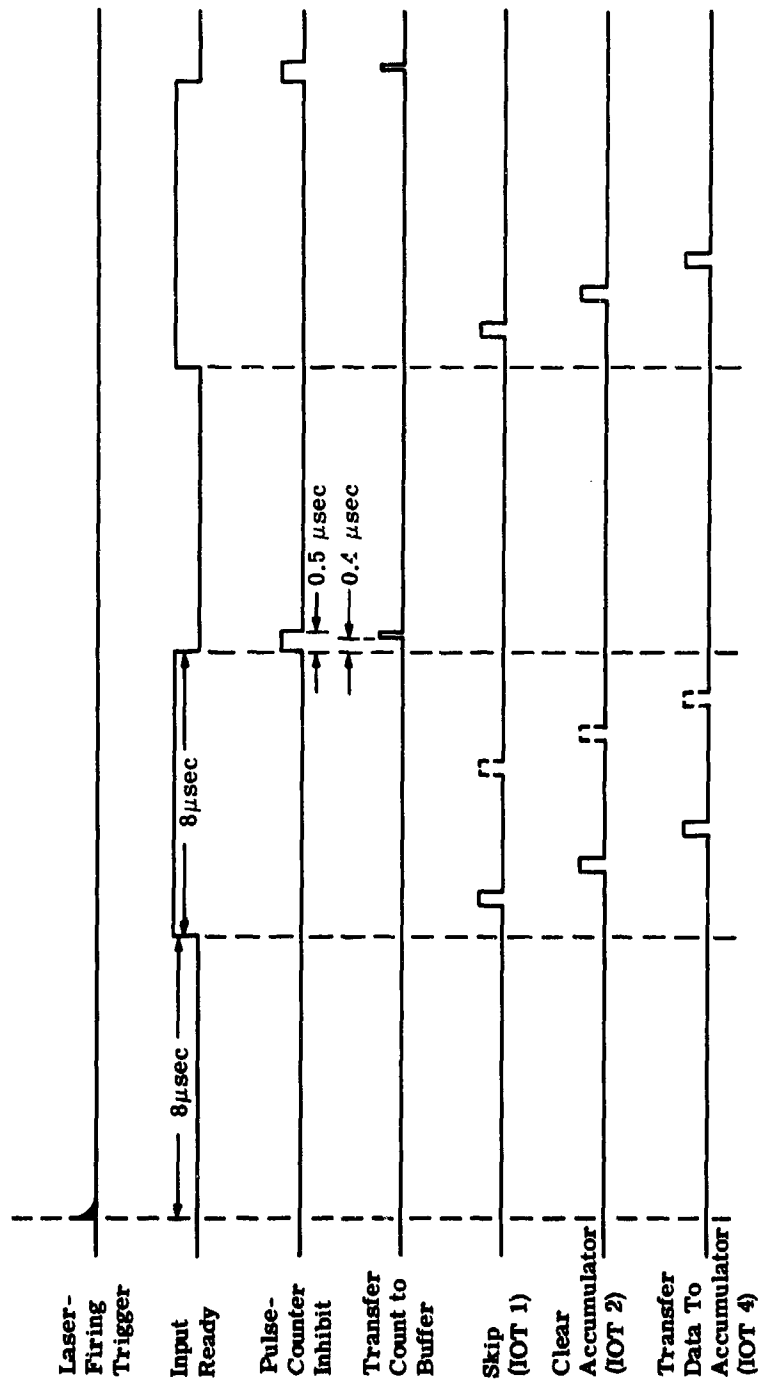
20

FIGURE 5. LASER INTERFACE TIMING. Earliest data transfer to PDP-8/I occurs 2.5 μsec after start of input ready cycle. Latest possible data transfer to PDP-8/I occurs 1 1/2 μsec before end of input ready cycle.

In the present application, it was found convenient to use IOP 1 (modified as described below) to activate the SKIP pin. IOP 2 is used to clear the PDP-8/I accumulator. Data words are transferred into the accumulator from the interface buffers by IOP 4.

When the computer comes to the IOT instruction, it issues a programmed device code which is detected by a W103 device selector (see the Logic Handbook [13]). If the correct code is present, then the IOP pulses are gated, by the W103, to the interface. The gated IOP pulses are designated IOT pulses in keeping with the notation used in the Small Computer Handbook [12].

IOT 1 is applied to the SKIP gate shown in figure 4. Activation of this gate during the time that the last stage of the ALTITUDE RESOLUTION/TIMING counter is in the "1" state produces a positive-going pulse that is applied to the SKIP pin on the PDP-8/I. IOT 2 is similarly gated to the CLEAR ACCUMULATOR pin, and IOT 4 is used to transfer data from the interface buffers to the PDP-8/I accumulator (fig. 4).

When using programmed data transfers (which require the least amount of interfacing), the DEC PDP-8/I computer does not wait for an input but must be in a "skip-loop" (see the DEC Small Computer Handbook [12]). Therefore, because there is no synchronization between the interface transfer rate and the computer cycle rate, it is not known exactly when a given pulse count is transferred from the buffer register to the PDP-8/I accumulator (AC). At first, this might seem disturbing until it is realized that, since the interface is the control element from the standpoint of time origin and resolution, it is only required that the computer accept each (interface-determined) pulse count (and nothing else) in its memory. It is not important exactly when, with respect to the interface time base, a given pulse count was taken from the buffer register.

The following analysis shows that the PDP-8/I is completely acceptable from this viewpoint. There are, in fact, several methods of making the PDP-8/I compatible with the interface. The input routine chosen is as follows: (See sec. 5.6 for an explanation of the program.)

Location	Contents	Time (μsec)
INPUT?	IOT YY X	4.25
NO — GO BACK	JMP INPUT	1.50
YES — STORE	DCAIZ TEMPO	4.50
LAYERS?	ISZ NEGLAY	3.00
NO — RETURN	JMP INPUT	1.50

Assuming that the computer is now in the "skip-loop" (jumping back and forth between INPUT and NO), there are two cases to consider:

(1) A SKIP pulse is not produced because the INPUT READY level is not present at the SKIP gate. In this case, the time between IOT 1 pulses (and transfers to the accumulator by the IOT 4 pulses) is 5.75 μsec.

(2) A SKIP pulse is produced; in other words, the interface is ready to transfer a data word to the PDP-8/I memory. In this case the time between inputs is 13.25 μsec.

If we keep these two input rates in mind and remember that transfers to the memory occur only when a SKIP pulse is generated (i.e., when the INPUT READY level and an IOT 1 pulse are both present at the SKIP gate), we see that we will always have one—and only one—input to the memory for each 16-μsec interval at the interface.

Note that, although meaningless inputs will occur to the accumulator (not the memory) when the INPUT READY level is not present, the accumulator is always cleared by the CLEAR ACCUMULATOR pulse before a "real" input is taken.

We must also be sure that a transfer from the buffers to the AC does not occur at the same time that an interface buffer transfer (pulse counter to buffer register) is taking place. The following argument shows that this will not happen. The buffer transfer always occurs on the 1 to 0 transition of the last flip-flop of the ALTITUDE RESOLUTION/TIMING counter and the first such transfer is 16 μsec after the laser fires. Assume that an input to the AC could occur at the same time and consider the two possible cases:

    (a) The previous IOT 1 pulse produced a SKIP pulse (i.e., an input). This means that it came 13.25 μsec before the assumed pulse. From figure 5, however, it is seen that this would occur when the INPUT READY level was not present, which is not possible. Therefore, this possibility must be excluded.

    (b) The previous IOT 1 pulse did not produce a SKIP pulse. This however, would mean that it came 5.75 μsec before the assumed pulse. Since 5.75 μsec is less than 8.0 μsec, the IOT 1 pulse would have occurred while the INPUT READY level was present and would, of course, produce a SKIP pulse; this conflicts with the assumption.

Therefore, it is impossible to generate an input to the AC while the buffers are receiving a transfer from the pulse counter (although the restrictions on all of the cycle times should be apparent).

The analysis given here shows that the PDP-8/I is an ideal computer for use with the LIDAR system. Although this report considers only programmed data transfers, the single-cycle data-break mode of operation can also be used. This requires more interfacing but is worth the expense because data transfer rates of 1.5 μsec per word (atmospheric layers of 0.22 km) can be achieved.

5.6. PDP-8/I COMPUTER PROGRAM

This section presents a program written for the Digital Equipment Corporation's PDP-8/I computer and intended for use with the LIDAR system described in this report. For the mean-

ing of all mnemonic codes, and an understanding of what each PDP-8/I instruction represents, the Digital Equipment Corporation's Small Computer Handbook [12] should be consulted. The program was assembled with the PAL III Symbolic Assembler.

Locations 0002-0010 and 0020-0026 are used for storage of constants, parameters that may be varied, and indirect addresses. The program stores the first interface "word" (un-reduced pulse count) in location 5001 and the first accumulated pulse count in location 1000. These addresses are given the symbolic tags UO and ALO respectively. ALO is stored in location 0002, and UO is stored in location 0020. Locations 0003 and 0004 are used for temporary storage of accumulated pulse-count addresses. Locations 0021 and 0022 are used for temporary storage of unreduced pulse-count addresses. Location 0005 contains the address (plus 1) of the most significant bits of an accumulated pulse count (tagged AMNI). The program given here is written for 100 atmospheric layers (of 2.4 km each). Location 0006 contains the negative (in octal) of the number of desired layers. Location 0007 contains the number of shots processed (K). In location 0024 we store an octal number that is equal to the first unreduced pulse-count address minus one. This number must be replaced in location 0010 (by the computer) after each laser firing. Location 0025 contains the number of shots to be processed.

Locations 0037-0053 contain instructions that set the contents of all permanent memory locations equal to zero.

Location 0054 contains an instruction that sets K = 0 when preparing for a new series of laser firings.

Locations 0055-0067 Contain instructions that set the initial addresses (both unreduced and accumulated) for each laser shot.

Locations 0070-0074 contain the input routine. The input instruction is in location 0070 and is described in section 5.5 in the discussion of the PDP-8/I interface. Location 0071 contains a jump instruction that keeps the PDP-8/I in a SKIP loop until an input has been taken. Location 0072 contains an instruction that deposits the unreduced pulse count in the appropriate temporary storage location. This (DCA IZ) is a very powerful instruction. It uses indirect addressing and the auto-indexing properties of memory locations 0010-0017 in the PDP-8/I (see the Small Computer Handbook [12]). The instruction in location 0073 checks to make sure that all layers have been taken for each shot.

The input routine presented here results in the maximum data transfer rate possible when programmed data transfers are used.

Locations 0075-0102 contain instructions that restore constants for the next laser firing.

Location 0103 may contain a halt instruction (7402) if it is necessary to inspect each laser shot.

Locations 0104-0116 contain instructions that calculate a pulse count, check for least significant bit overflow, and then store the result in the appropriate memory location (instructions 0117 and 0130).

Locations 0120-0127 contain instructions that check for a most significant bit overflow (this would require an accumulated total of $2^{23} - 1$ pulses in a given bin), which would require an immediate typeout of the data.

Locations 0131-0153 contain instructions that set up for the next layer for the shot being processed and check to see if all layers have been stored.

Locations 0154-0166 contain instructions that check to see if the required number of shots have been processed. If "no," another laser firing is required. If "yes," the data may be typed out.

Operation of the program proceeds as follows. The program is loaded into memory using the BIN loader and the ASR-33 teletype reader provided with the PDP-8/I. The program is started at location 0037 and will enter the skip-loop at locations 0070-0071, waiting for the laser to be fired. When the laser is fired, the input is taken, as shown in figure 5.

When the prescribed number of layers has been taken, the computer begins the calculation and storage of accumulated pulse counts (this takes approximately 2 msec), after which the computer will return for another laser firing. It is necessary to make sure that the INPUT READY level drops out before the computer finishes this section of the program and returns for an input. This is governed by the one-shot that is activated by the laser trigger pulse. The period of this one-shot should be set for about 1.8 msec. This assures that 100 layers can be taken for each shot. When the prescribed number of shots (usually 100) has been processed, the computer will halt at location 0164. The data may then be typed out.

Unless a halt instruction (for single-shot inspection of each laser pulse) is included at location 0103, the operator need wait only for all 100 shots to be taken. If the halt instruction is included, the operator must start the computer at location 0104 if the shot is acceptable, or at location 0055 if the shot must be discarded.

Data typeout is achieved by using the Digital 8-6-U Sym Octal Dump Routine which is included here. An octal-to-decimal conversion routine would, of course, facilitate data reduction.

24

```
/LIDAR EXPERIMENT - MT. HALEAKALA OBSERVATORY
*2/STORAGE
ALO,      1000 /ADD. OF L.S.B. OF 1ST APC
ALF,      0000 /ADD. OF L.S.B. OF JTH APC
AMJ,      0000 /ADD. OF M.S.B. OF JTH APC
AMNI,     1310 /ADD. OF M.S.B. OF LAST APC+1
          7634 /-LAYERS (FOR 100 DEC.)
K,        0000 /NO. OF SHOTS PROC.
          5000 /ADD. OF 1ST UPC-1
*20
UO,       5001 /ADD. OF 1ST UPC
UJ,       0000 /ADD. OF JTH UPC
UJI,      0000 /ADD. OF (J+1)TH UPC
LAYERS,   0144 /NO. OF LAYERS (100 DEC.)
SETO10,   5000 /SET LOC.010 FOR NEXT SHOT
SHOTS,    0144 /NO. OF SHOTS WANTED
/BEGIN INT. SETUP
*37
START, CLA CLL /BEGIN SET (APC) =0
       TAD ALO
       DCA ALJ
       CLA
       DCA I ALJ
       TAD ALJ
       IAC
       DCA ALJ
       TAD ALJ
       CIA
       TAD AMNI
       SZA /ALL BINS CONTAIN ZERO ? YES-SKIP
       JMP 042 /NO REPEAT
       DCA K /SET K=0
       TAD ALO /SET INT. ADD. FOR PERM. STOR.
       DCA ALJ
       TAD ALO
       IAC
       DCA AMJ
       TAD UO /SET INT. ADD. FOR INP.
       DCA UJ
       TAD UO
       IAC
       DCA UJI
       CLA CLL /READY FOR INP.
INPUT, 6437 /SKIP NXT. INST. IF INTERFACE READY
       JMP 070 / GO BACK IF NOT READY
       DCA I Z 010 /DEPOSIT INP. IN TEMP. STORAGE
       ISZ 006 /SKIP IF ALL INP. TAKEN
       JMP 070 /GO BACK FOR MORE INP.
       CLA CLL
       TAD LAYERS
       CIA
       DCA 006 /RESTORE - LAYERS
       TAD SETO10
       DCA 010 /RESTORE (010)
       NOP /CAN BE HALT IF LASER PROB.
       CLA CLL
       TAD I UJ /BEG. CALC. OF P.C.
       CIA
       TAD I UJI
       NOP
       NOP
       CLL
       TAD I ALJ
```

```
                    SZL /SKIP IF NO L.S.B. OVFL.
                    SKP
                    JMP STLSB
                    DCA I ALJ /STORE L.S.B.
                    IAC
                    CLL
                    TAD I AMJ
                    SZL /SKIP IF NO M.S.B. OVFL.
                    HLT /STOP-MUST TYPE OUT
                    DCA I AMJ /STORE M.S.B.
                    CLA
                    SKP
              STLSB,DCA I ALJ /STORE L.S.B.
                    TAD UJ /SET UP FOR NXT. LAYER
                    IAC
                    DCA UJ
                    TAD UJI
                    IAC
                    DCA UJI
                    TAD ALJ
                    IAC
                    IAC
                    DCA ALJ
                    TAD AMJ
                    IAC
                    IAC
                    DCA AMJ
                    TAD ALJ
                    CIA
                    TAD AMNI
                    SZA /HAVE ALL LAYERS BEEN STORED?
                    JMP 104 /NO GO BACK FOR MORE
                    TAD K
                    IAC
                    DCA K
                    TAD K
                    CIA
                    TAD SHOTS
                    SZA /HAVE ALL SHOTS BEEN TAKEN?
                    SKP
                    HLT /YES-READY TO TYPE OUT DATA
                    CLA
                    JMP 055 /NO-GO BACK FOR MORE SHOTS
              /END OF DATA ACQUISITION PROGRAM
                $
```

PDP-8/I Octal Dump Routine

Address		Four Data Words		
7400	7200	7404	3256	7402
7404	7404	7040	1256	3257
7410	5213	2260	5226	1265
7414	3260	4247	1256	4661
7420	1265	3247	1264	4241

7424	2247	5222	7200	1656
7430	4661	1264	4241	2256
7434	2257	5211	4247	7402
7444	5243	7200	5641	0000
7450	7200	1263	4241	1262
7454	4241	5647	74E6	7741
7460	7774	7466	0212	0215
7464	0240	7774	7431	3311
7470	1265	3310	1311	7004
7474	7004	7006	3311	1311
7500	0313	1314	4712	1311
7504	2310	5274	7200	5666
7510	0000	0000	7441	0007
7414	0260			

1. Load with BIN loader and ASR-33 teletype reader.

2. Set 7400 in switch register and press Load Address key.

3. Set FWA in switch register and press Start key.

4. Set LWA in switch register and press Continue key.

6
## EXPERIMENTAL RESULTS OBTAINED WITH THE DATA-ACQUISITION SYSTEM

The LIDAR data-acquisition system described in this report has been fabricated, calibrated, and used, in conjunction with the Mount Haleakala pulsed ruby laser, to obtain preliminary atmospheric backscattering profiles. These profiles were made from the standpoint of system checkout rather than for the purpose of gathering atmospheric data. Neither of the shutters required for meaningful pulse-counting measurements (see secs. 2 and 4.3 of this report) was in operation.

The method used was to: (a) operate the laser at very low power levels, (b) fire into the atmosphere and observe the analog output on an oscilloscope, (c) repeat (b) while inserting neutral-density filters in front of the PMT so that the signal was attenuated to the pulse counting level. An example of the technique is shown in figure 6.

The photographs in figure 6 show the overlap of the transmitter and receiver beams at an altitude of about 3 km. The signal then decreases with altitude in the expected manner. A slight "valley" is seen at about 10 μsec; this is due to multiple scattering between the trans-
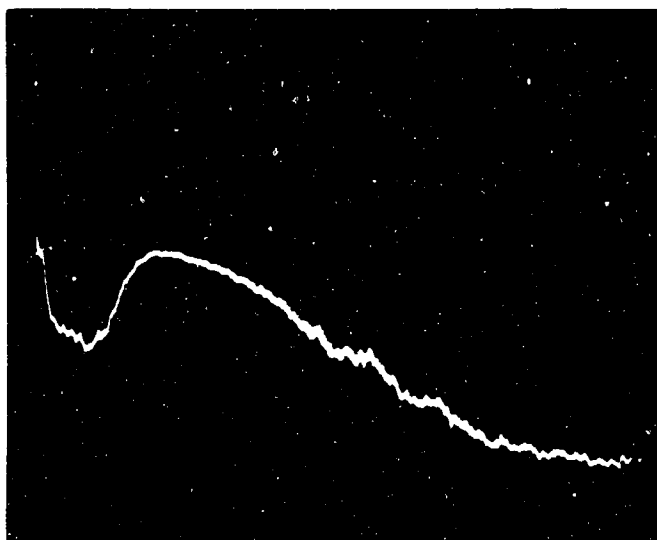
(a) Unattenuated Return: 10 μsec (1.5 km) per Division. (The Vertical Scale is Logarithmic.)
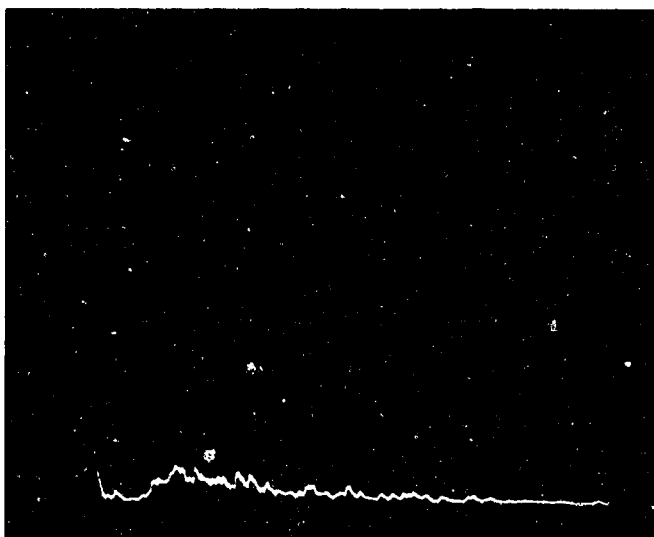
(b) Return Attenuated with Neutral-Density Filters

FIGURE 6. LOWER ATMOSPHERIC BACKSCAT-TERING PROFILES

28

mitter and receiver beams at low altitudes. The noise spike seen at the beginning of the sweep is caused by light from the outgoing Q-switched pulse being "seen" by the secondary mirror of the 48-in. receiver. This effect has now been completely eliminated by installing light baffles. Figure 6b represents an intermediate stage between "current" and pulse counting. The PMT load was 500 Ω when these pictures were taken. A load of 50 Ω was used for pulse-counting measurements.

Table V gives the results obtained for 100 shots, using the complete digital data-acquisition system. The magnitude of the signal return is not meaningful because no system calibration was performed and, as stated above, the laser was operated at low power levels and neutral-density filters were installed in front of the PMT. The pulse count for the first layer is omitted since the first word loaded into memory on each shot is meaningless (actually, it will be the last word of the previous shot) and, therefore, the first difference (i.e., the net pulse count for the first layer) will also be meaningless. The noise level is rather high primarily because the PMT was uncooled. A 50-Å interference filter was used, but some fluorescence contamination was obviously present. The data is plotted in figure 7. For comparison, a predicted curve (con-

TABLE V. ATMOSPHERIC PULSE-COUNTING DATA: 30 APRIL AND 26 JUNE 1969 (100 SHOTS)

Layer	Altitude (km)	Total Counts	Signal Counts per Shot[*]
1	2.5	-	-
2	5.0	604	5.86 ± 0.24
3	7.5	413	3.95 ± 0.20
4	10.0	208	1.90 ± 0.14
5	12.5	116	0.98 ± 0.10
6	15.0	70	0.52 ± 0.07
7	17.5	46	0.28 ± 0.05
8	20.0	39	0.21 ± 0.05
9	22.5	21	-
10	25.0	24	-
11	27.5	15	-
12	30.0	19	-
13	32.5	13	-
14	35.0	10	-
15	37.5	23	-
16	40.0	15	-

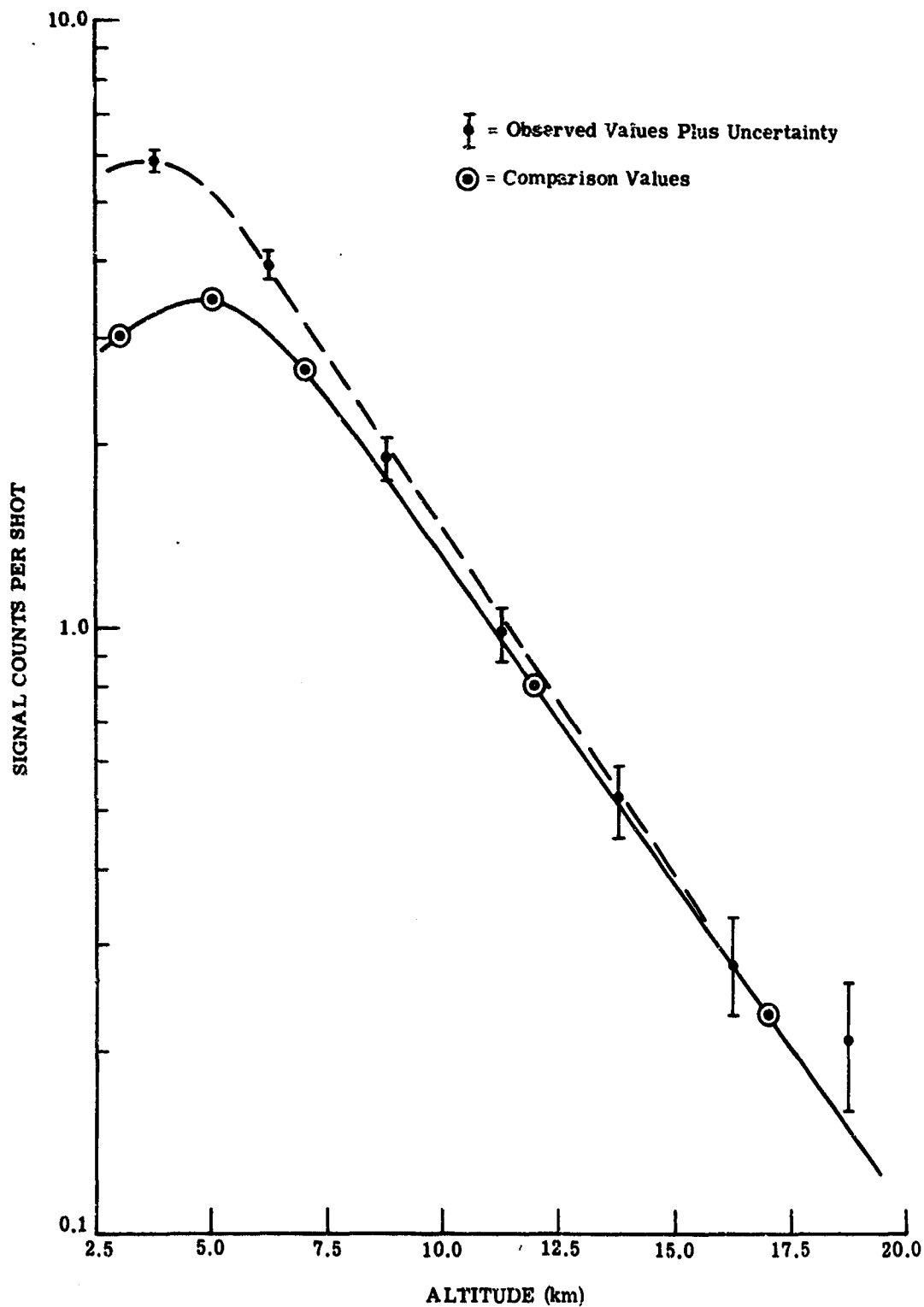[*]Obtained by subtracting the "background" as determined by layers 9-16 and dividing the result by 100.

FIGURE 7. AN ATMOSPHERIC (PULSE-COUNTING) PROFILE

structed from table I) for a receiver field of view of 0.2 mrad is also shown. The two curves scaled to agree at 17.0 km. It is seen that the curves agree quite well from the standpoint of dependence upon altitude. It is obvious that the actual receiver field of view is greater than 0.2 mrad (which was verified by passing a star through the receiver field). Figure 6a also shows this to be the case. The pulse-counting profile shown in figure 7 agrees very well with the "current" profile shown in figure 6a.

7
CONCLUSIONS

The preliminary data presented in section 6 clearly demonstrates that the LIDAR digital data-acquisition system described in this report is operational from the standpoint of obtaining upper atmosphere backscattering profiles. The system is versatile (e.g., various altitude resolutions may be used, depending on the particular physical considerations) and relatively inexpensive, considering the potential yield of important scientific data. Since a digital computer is an integral part of the system, data reduction can be done in real time. For example, actual backscattering profiles can be plotted a few seconds after a group of shots has been fired into the atmosphere.

Upon installation of the required shutters, the Mount Haleakala LIDAR system will be used to obtain backscattering data from altitudes upwards of 100 km. An inspection of figure 3 (for the high quantum efficiency system) indicates that meaningful results may be obtained up to 120 km in reasonable time periods for the relatively high-repetition-rate Mount Haleakala system.

Appendix
DESCRIPTION OF CIRCUITS

This appendix describes the circuits shown in figure 4 in more detail. All components are Digital Equipment Corporation Flip Chip Modules installed in an H900 Mounting Panel.

A.1. ALTITUDE RESOLUTION/TIMING (Figure 8).

A trigger pulse from the laser firing circuit starts the CLOCK ENABLE one-shot (or delay), permitting 8-MHz clock pulses to enter the INTERFACE TIMING/ALTITUDE RESOLUTION binary counter. The TIMING/ALTITUDE counter is a divide-by-64 counter whose output stage, called the INPUT READY flip-flop, changes state every 8 μsec. Each complete cycle of the INPUT READY flip-flop represents one 2.4 km altitude layer.

The delay set in the CLOCK ENABLE one-shot determines how many layers will be observed for each laser firing. At the end of the delay, the TIMING/ALTITUDE counter flip-flops are reset to zero.

A.2. BUFFER-TRANSFER AND PULSE-COUNTER INHIBIT PULSES (Figures 9, 10, 11).

The transfer and inhibit pulses are generated from the one to zero transition of the INPUT READY flip-flop. The inhibit pulse is required to insure that the pulse-counter flip-flops are not changing state when a buffer transfer occurs. Because of the propagation delays of the later stages in the pulse counter, the input stages must be inhibited for 0.5 μsec. The TRANSFER pulse is delayed to occur near the end of the INHIBIT pulse.

A.3. DATA TRANSFERS TO THE PDP-8/I (Figure 12)

Figure 11 shows the circuits used to effect data transfers from the interface to the PDP-8/I. The basic concepts involved are discussed in sections 5.5 and 5.6.
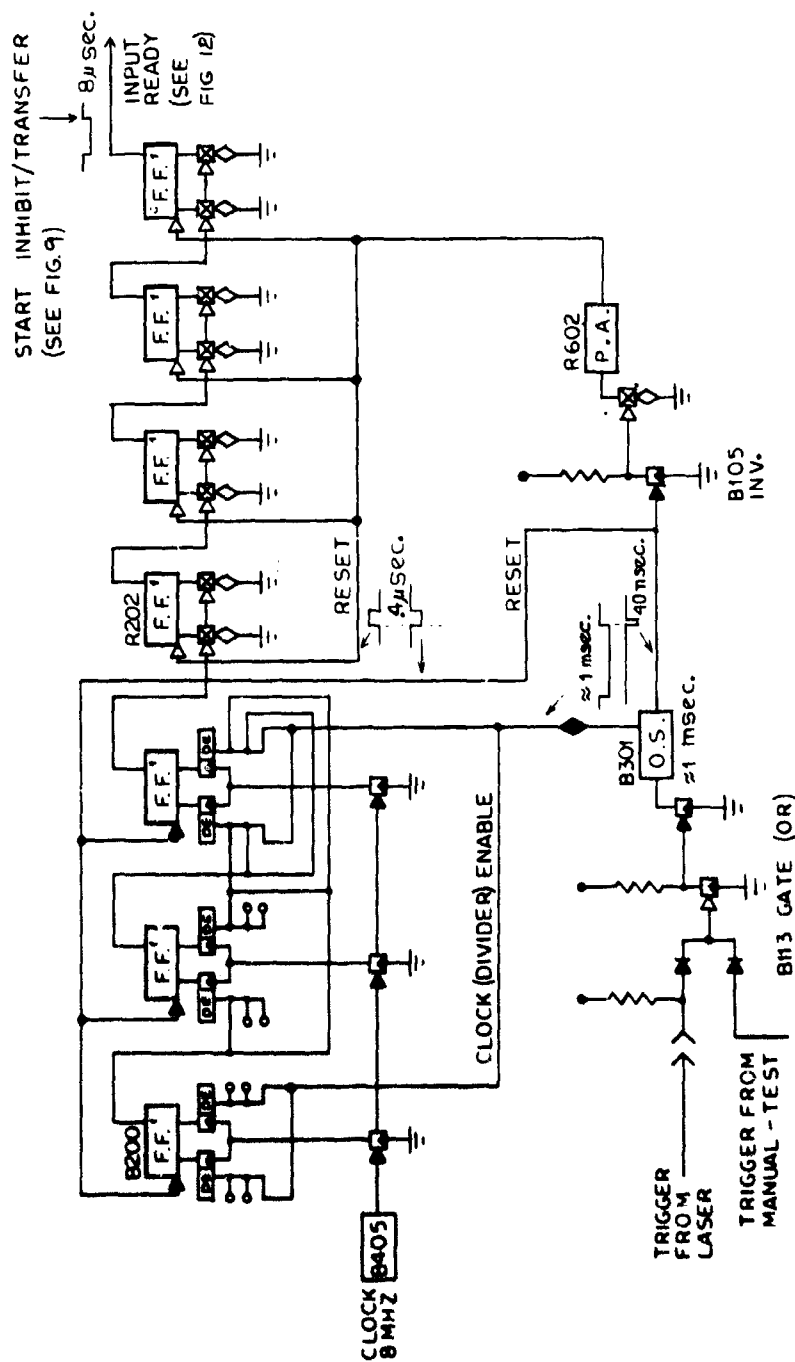
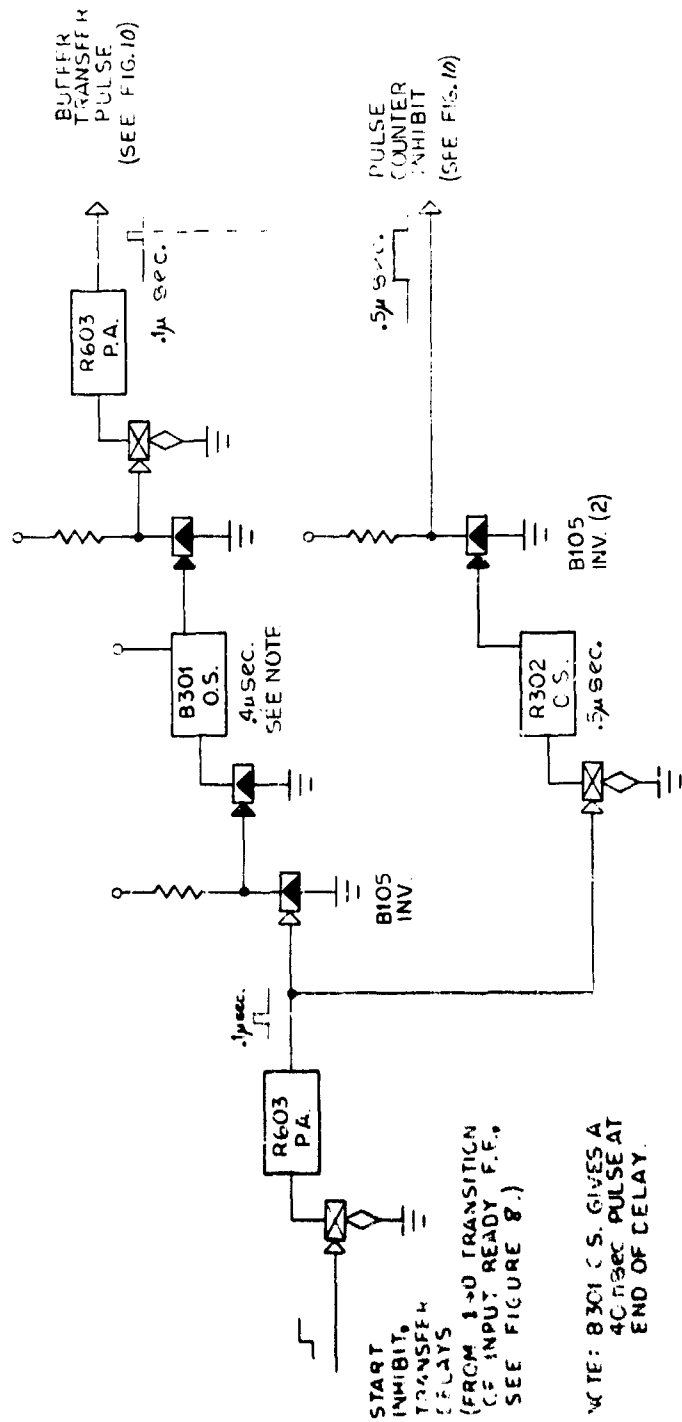FIGURE 8. LASER INTERFACE: ALTITUDE RESOLUTION/TIMING

34

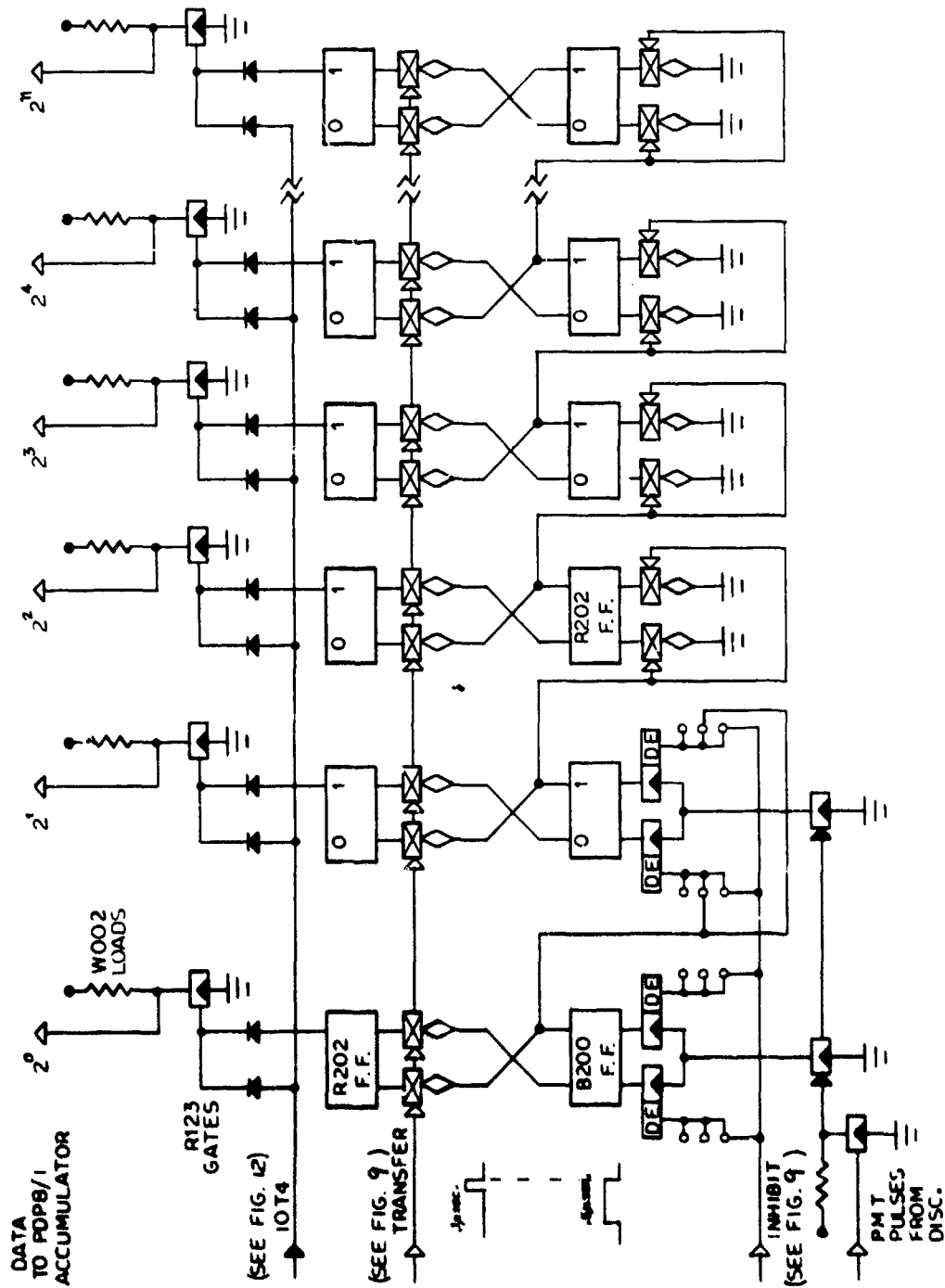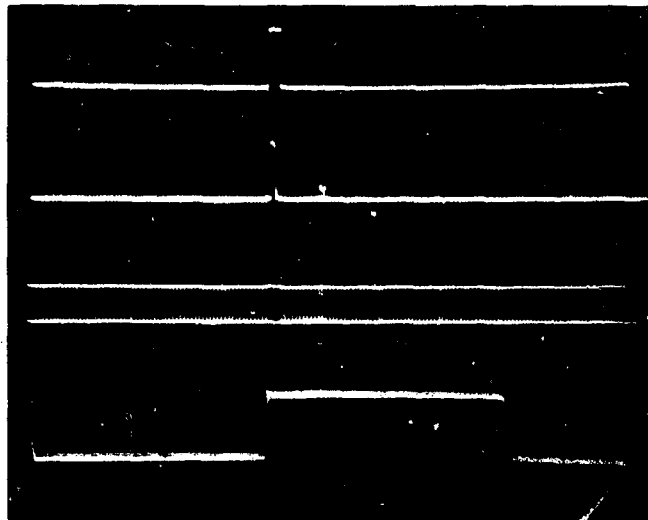**FIGURE 9. LASER INTERFACE: BUFFER-TRANSFER PULSE AND PULSE-COUNTER INHIBIT DELAYS**

35

FIGURE 10. LASER INTERFACE: DATA IOT GATES, BUFFER REGISTER, PULSE COUNTER

Time base: 2 μsec per division
First trace: Pulse-counter inhibit pulse
Second trace: Buffer-transfer pulse
Third trace: Output of first stage of pulse counter
Fourth trace: INPUT READY flip-flop

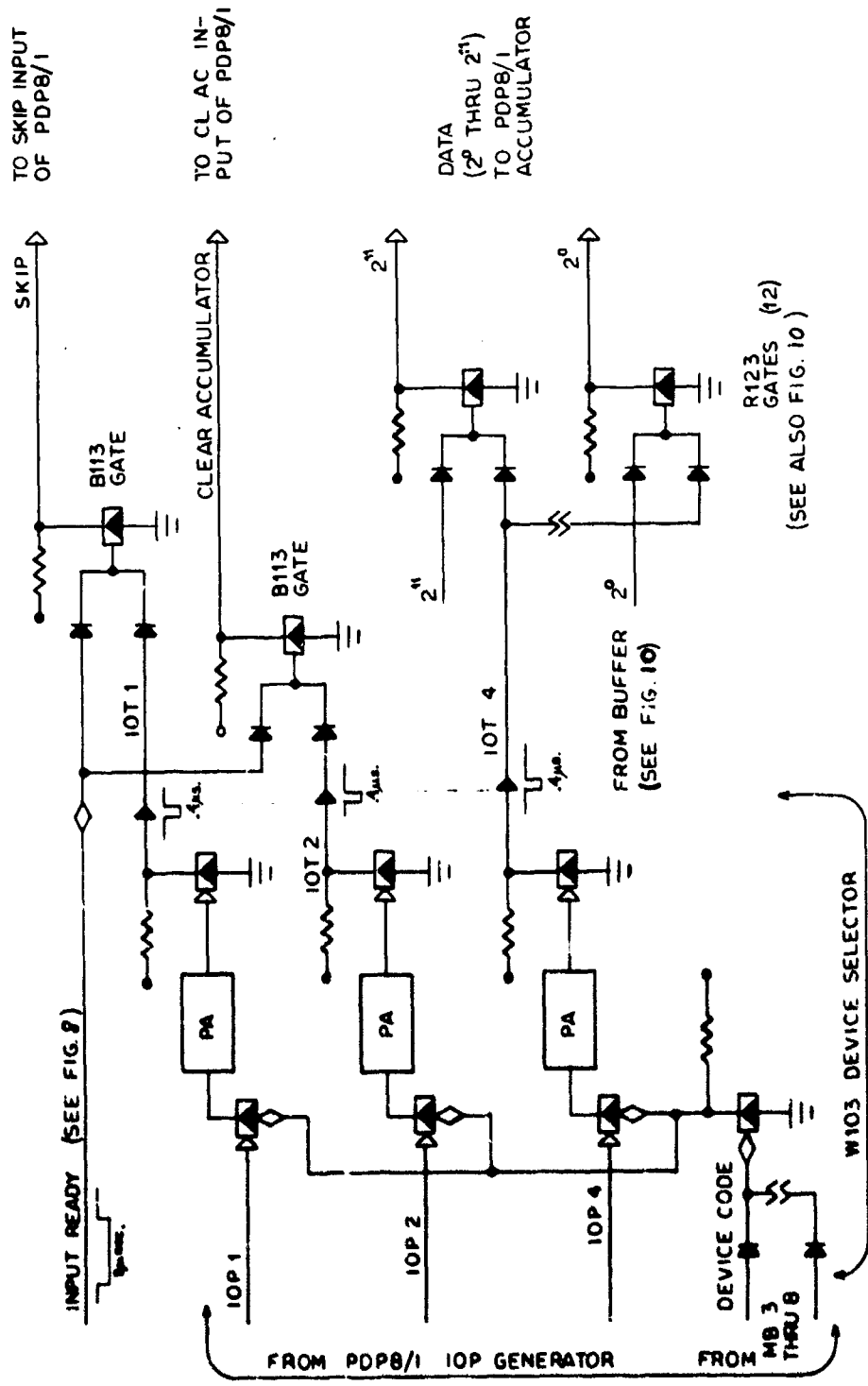FIGURE 11. TRANSFER AND INHIBIT PULSE OPERATION

37

FIGURE 12. LASER INTERFACE: PDP-8/I INPUT-OUTPUT TRANSFERS

REFERENCES

1. G. Fiocco and G. Colombo, J. Geophys. Res., Vol 69, p. 1795 (1964).

2. W. C. Bain and M. C. W. Sandford, J. Atmospheric Terrest. Phys., Vol. 28, p. 543 (1966).

3. G. S. Kent et al., J. Atmospheric Terrest. Phys., Vol. 29, p. 169 (1967).

4. P D. McCormick et al., Nature, Vol. 215, p.1262 (1967).

5. P. D. McCormick, Doctoral Thesis, University of Maryland, College Park, (1967).

6. P. D. McCormick et al., J. Atmospheric Terrest. Phys., Vol. 31, p. 185 (1969).

7. C. A. Northend et al., Rev. Sci. Instr., Vol. 37, p. 393 (1966).

8. U. S. Standard Atmosphere: 1962, U. S. Government Printing Office, Washington, D. C.

9. C. W. Allen, Astrophysical Quantities, University of London, The Athlone Press (1963).

10. P. D. McCormick, J. Atmospheric Terrest. Phys., Vol. 31, p. 793 (1969).

11. R. T. Bettinger, University of Maryland, College Park, Dept. of Physics and Astronomy, Technical Report 617 (1966).

12. Digital Equipment Corporation Small Computer Handbook, Maynard, Mass., (1968).

13. Digital Equipment Corporation Logic Handbook, Maynard, Mass., (1968).

DOCUMENT CONTROL DATA - R & D

(Security classification of title, body of abstract and indexing annotation must be entered when the overall report is classified)

1 ORIGINATING ACTIVITY (Corporate author) Willow Run Laboratories, Institute of Science and Technology, The University of Michigan, Ann Arbor, Michigan	2a. REPORT SECURITY CLASSIFICATION Unclassified
	2b GROUP

3 REPORT TITLE

Report of the Mount Haleakala Observatory: A LIDAR DATA-ACQUISITION SYSTEM USING AN ON-LINE DIGITAL COMPUTER

4 DESCRIPTIVE NOTES *(Type of report and inclusive dates)*

5 AUTHOR(S) *(First name, middle initial, last name)*

Paul D. McCormick and H. David Hultquist

6 REPORT DATE February 1970	7a. TOTAL NO. OF PAGES vi + 41	7b NO. OF REFS 13
8a. CONTRACT OR GRANT NO. DAHC-15-68-C-0144 b PROJECT NO c. d.	9a. ORIGINATOR'S REPORT NUMBER(S) 1386-29-T 9b OTHER REPORT NO(S) *(Any other numbers that may be assigned this report)*	

10 DISTRIBUTION STATEMENT

This document has been approved for public release and sale; its distribution is unlimited.

11 SUPPLEMENTARY NOTES	12. SPONSORING MILITARY ACTIVITY Advanced Research Projects Agency, Department of Defense, Washington, D. C.

13 ABSTRACT

This report describes the design and operation of a data-acquisition system which uses digital circuits and an on-line PDP-8/I computer for real-time data processing to make upper atmospheric LIDAR measurements. The system is presently being used with the high-power pulsed ruby laser which has recently been installed at the Mount Haleakala Observatory, Maui, Hawaii.

The report discusses the basic concepts involved in obtaining LIDAR measurements of atmospheric backscattering. Expected signal returns for both the "current" (lower atmosphere) and pulse-counting (upper atmosphere) cases are calculated. Noise and background sources are considered in detail, and the statistical nature of the upper atmospheric experiments is emphasized. Detailed circuit diagrams for the data acquisition system and a LIDAR data-acquisition program for the PDP-8/I computer are also included.

Preliminary data obtained with the LIDAR system is presented and compared with prediction. It is concluded that the Mount Haleakala LIDAR system will be capable of producing high-precision atmospheric backscattering profiles to altitudes of the order of 100 km.

KEY WORDS	LINK A		LINK B		LINK C	
	ROLE	WT	ROLE	WT	ROLE	WT
Data acquisition						
LIDAR						
On-line computer						
Atmospheric backscattering						
Lasers						
Atmosphere						
Observatories						
Optical data						